

### Journal of Stress Analysis

Vol. 8, No. 2, 2023-24, 1-17



ORIGINAL RESEARCH PAPER

# An Efficient Optimal Analysis Approach to Reliability-Based Design Optimization of Symmetric Skeletal Structures

Hashem Mehanpour, Seyed Rohollah Hoseini Vaez\*

Department of Civil Engineering, Faculty of Engineering, University of Qom, Qom, Iran.

### Article info

### Article history: Received 27 September 2023 Received in revised form 23 December 2024 Accepted 01 January 2024

Keywords:
Optimal analysis
Symmetric skeletal structures
Uncertainty of parameters
Metaheuristic algorithms
Probability of failure

#### Abstract

The properties of symmetrical structures can cause the optimal analysis of these types of structures to have greater ease, speed, and accuracy. It also saves space for storing large-scale matrices. Reducing these computational costs is very useful in structural problems that require frequent analysis of the specific structure. One of the problems that need repeated structural analysis is Reliability-Based Design Optimization (RBDO) of structures utilizing meta-heuristic algorithms. This study presents an efficient approach to the optimal analysis of symmetric skeletal structures. With a systematic and programmable procedure, this approach extracts the submatrices whose dimensions are half or less than half of the main structure's stiffness matrix. Then, the inverse of the stiffness matrix can be determined by calculating the inverse of submatrices whose dimensions are half or less than half the dimensions of the main structure's stiffness matrix. Two symmetric benchmark structures with general loading were investigated to assess the proposed approach to solving the RBDO problem. The proposed approach reduces the dimensions of matrices that must be inverted, and the computational time for solving the RBDO problem using Enhanced Vibrating Particle System (EVPS) algorithms, compared to the direct method.

### Nomenclature

RBDO	Reliability-Based Design Optimization	EVPS	Enhanced Vibrating Particle System
MCS	Monte Carlo Simulation	K	Stiffness matrix of the structure
$\mathbf{F}$	Vector of external loads	U	Vector of nodal displacements
E	Young's modulus	I	Moment of inertia
A	Cross-sectional area	$\mid \mid F_y \mid$	Yield stress of material
$\gamma$	Weight per volume of material	R	Maximum drift index
$R_l$	Inter-story drift index	d	Vector of deterministic design variables
β	Reliability index	$P_s$	Probability of safety
$\mathbf{T}$	Transformation matrix	$\parallel g_i$	i-th deterministic constraint
A, B, X	Submatrices of the stiffness matrix	$\mid \mid f \mid$	Objective function (typically the struc-
and $\mathbf{Q}$			ture's weight)

<sup>\*</sup>Corresponding author: S.R. Hoseini Vaez (Assistant Professor)

E-mail address: hoseinivaez@qom.ac.ir doi 10.22084/JRSTAN.2023.27860.1244

ISSN: 2588-2597



$\mathbf{C}_1$ and	Intermediate matrices for inverse calcu-	$\phi_b, \phi_c$	Resistance reduction factors for bend-
$\mathbf{C}_2$	lation		ing and axial strength
$ \bar{g}_j $	Limit state function for the j-th proba-	$oldsymbol{\mu}_X, oldsymbol{\mu}_P$	Mean vectors of random variables $(\mathbf{X})$
	bilistic constraint		and random parameters $(\mathbf{P})$
$M_n$ and	Nominal bending and axial strength	$M_u$ and	Required bending and axial strength
$P_n$		$P_u$	
S1, S2	Groups of symmetric structures $(S1:$	$\sigma_j, \sigma_a$	Stress of the j-th member and allowable
	axis intersects members; S2: axis		stress
	passes through nodes)		
D1, D2, D11, D22, D33, D12, D13, D23		Submatri	ces for inverse calculation

### 1. Introduction

Numerical approaches, such as finite element analysis, are used to solve structural engineering problems, resulting in the construction of large stiffness matrices. For the static analysis of these structures, the inverse of large-scale matrices must be calculated. In some structural problems, approaches for reducing computational volume, problem size, and data volume for computer memory can be provided. It will decrease numerical errors and, as a result, increase calculating speed and convenience without reducing accuracy. Symmetrical structures, which have many applications in engineering, are one of these problems [1-7]. For the analysis of such structures, symmetry gives more information in addition to the basic information, which will be very beneficial. This additional information can be used for faster analysis and lower computational costs and errors. Several methods for optimal analysis of symmetric structures have been proposed by researchers. In these methods, using group theory, graph theory, and linear algebra, mainly the eigenvalue problems of symmetric structures are solved [8]. Group theory is used for block diagonalization of matrices [9-11]. In graph-theoretical methods, graph models of planar and spatial structures are divided into appropriate substructures. A suitable algorithm for applying boundary conditions and forming desirable substructures to solve particular problems is presented [12,13]. Many approaches of the last two decades are based on linear algebra with block-diagonal matrices [14-16]. In these approaches, canonical forms are used for the efficient calculation of matrix eigenvalues [17-19]. These approaches have been applied to problems such as combinatorial optimization, free and forced vibration of structures, determining critical loads of frames, ordering and partitioning of structures, the vibration of the mass-spring system, and eigenvalue calculation of the Laplacian matrix of a symmetric graph [20,19,21-23. Matrix decomposition and block diagonalization of these matrices are commonly used to provide efficient eigensolutions in structural mechanics problems [24,25]. Previous studies and reviews on this issue are about the problem of determining the critical loads of frames, free vibration of structures, the partitioning of finite element models, the optimal order and vibration

of systems consisting of mass and spring, and the calculation of the eigenvalues of the Laplacian matrix of graphs with different forms of symmetry. Most of these studies are concerned with computing the eigensolution of regular structures and graphs. Fewer studies have been carried out on the static analysis of symmetric structures. The matrix linear algebra approach is used for linear static analysis, and the graph theory approach is not used for such problems.

The efficiency of optimal structural analysis methods is more applicable when the structure is large-scale and has very high degrees of freedom and also when a significant number of structural analyses must be repeated. Solving nonlinear problems is one of the problems that requires frequent structural analysis. In fact, in solving non-linear problems, usually with different assumptions and methods, the problem becomes several repeated linear problems. After converting the nonlinear problem into several repeated linear problems, the efficient proposed method presented in this article can be used to solve them. The reliability-based design optimization (RBDO) problems integrated with meta-heuristic algorithms are one of the problems that require repeated structural analysis. There are several methods to solve RBDO problems[26]. These methods include two-level [27], decoupled [28], and mono-level [29] methods. The two-level method is the most suitable for complex and nonlinear problems among these methods. Other advantages of this method include no dependence on the design point and no need for limit state function derivatives [30]. This method can be used to solve any RBDO problem with any constraint because of its generality. The Monte Carlo simulation (MCS) method, which is one of the most general, widely used, and accurate methods for evaluating probabilistic constraints, can also be utilized in the inner loop [31-33]. A given structure must be analyzed several times in order to solve the RBDO problem, utilizing the double-loop method and the metaheuristic algorithm. The high number of iterations, population size, the number of independent runs of the meta-heuristic algorithm in the outer loop, and the high number of MCS sample points in the stage of assessing the structure's reliability in the inner loop necessitate these iterative analyses.

This study provides an approach for static analysis on symmetric skeletal structures, reducing computational time and memory space. The proposed approach calculates the inverse of the main structure's stiffness matrix by calculating the inverse of sub-matrices obtained from the halved model of the structure. The efficiency of the proposed approach is evaluated by comparing the analysis time of symmetrical frames with different numbers of bays and stories using two different methods (the direct method and the proposed method). Furthermore, RBDO for two symmetric skeletal structures (a 3-bay 15-story frame and a 200bar planar truss) is investigated. In these problems, the MCS approach is employed for reliability assessment, and an enhanced vibrating particle system (EVPS) algorithm is used for optimization. The results indicate that structural analysis using the proposed approach reduces the computational time and the data volume stored in the memory while maintaining the accuracy of the answers when compared to the direct method. Additionally, reducing the time required for structural analysis, which is a time-consuming procedure in solving the RBDO problem using meta-heuristic algorithms, leads to a significant reduction in calculations of the optimal design.

Following is an overview of the rest of the research. In Section 2, theorems for the inverse calculation of matrices of specific forms are presented. Section 3 presents the step-by-step procedure for optimal analysis of symmetric structures. RBDO formulation and EVPS optimization algorithm are briefly described in section 4. Section 5 provides computational time for static analysis of frame structures with different bays and stories. Two benchmark symmetric skeletal structures are shown in Section 6, including a 3-bay 15-story frame and a 200-bar planar truss. The conclusions are presented in the final section.

### 2. The Theorems for Inverse Calculation of Matrices with the Particular Form

Two specific forms of the matrix (referred to as  $\mathbf{K}_1$  and **K**<sub>2</sub>) are defined in this section, and their inverse caloperations, and simplification, Eq. (7) can be proved.

culations are proved using Theorems 1 and 2 [17]. The inverse of these two particular forms is used for the inverse calculation of stiffness matrices of symmetric structures in Section 3.

### 2.1. Theorem 1

Assume that the matrix  $\mathbf{K}_1$  is in the form of Eq. (1).

$$[K_1] = \begin{bmatrix} [A]_{n \times n} & [B]_{n \times n} \\ [B]_{n \times n} & [A]_{n \times n} \end{bmatrix}_{2n \times 2n}$$
(1)

where n is the dimension of the matrices **A** and **B**. When the matrices  $\mathbf{A} + \mathbf{B}$  and  $\mathbf{A} - \mathbf{B}$  are invertible (nonsingular matrices), the inverse of the matrix  $\mathbf{K}_1$  is obtained from Eq. (2).

$$[K_1]^{-1} = \begin{bmatrix} [D_1]_{n \times n} & [D_2]_{n \times n} \\ [D_2]_{n \times n} & [D_1]_{n \times n} \end{bmatrix}_{2n \times 2n}$$
(2)

To calculate the matrices  $\mathbf{D}_1$  and  $\mathbf{D}_2$ , first, the matrices  $C_1$  and  $C_2$  are obtained from Eqs. (3) and (4), respectively. Then, the matrices  $\mathbf{D}_1$  and  $\mathbf{D}_2$  are obtained according to Eqs. (5) and (6), in turn.

$$C_1 = (A - B)^{-1} (3)$$

$$C_2 = (A+B)^{-1} (4)$$

$$D_1 = (\frac{1}{2})(C_2 + C_1) \tag{5}$$

$$D_2 = (\frac{1}{2})(C_2 - C_1) \tag{6}$$

Proof of Theorem 1: Because the inverse of a matrix is unique, it is sufficient to prove Eqs. (7) and (8) in order to prove this theorem.

$$[K_1][K_1]^{-1} = [I] \tag{7}$$

$$[K_1]^{-1}[K_1] = [I]$$
 (8)

According to Eq. (9), by replacement, algebraic

$$[K_{1}][K_{1}]^{-1} = \begin{bmatrix} A & B \\ B & A \end{bmatrix} \begin{bmatrix} D_{1} & D_{2} \\ D_{2} & D_{1} \end{bmatrix} = \begin{bmatrix} AD_{1} + BD_{2} & AD_{2} + BD_{1} \\ BD_{1} + AD_{2} & BD_{2} + AD_{1} \end{bmatrix}$$

$$= (\frac{1}{2}) \begin{bmatrix} A(C_{2} + C_{1}) + B(C_{2} - C_{1}) & A(C_{2} - C_{1}) + B(C_{2} + C_{1}) \\ B(C_{2} + C_{1}) + A(C_{2} - C_{1}) & B(C_{2} - C_{1}) + A(C_{2} + C_{1}) \end{bmatrix}$$

$$= (\frac{1}{2}) \begin{bmatrix} AC_{2} + AC_{1} + BC_{2} - BC_{1} & AC_{2} - AC_{1} + BC_{2} + BC_{1} \\ BC_{2} + BC_{1} + AC_{2} - AC_{1} & BC_{2} - BC_{1} + AC_{2} + AC_{1} \end{bmatrix}$$

$$= (\frac{1}{2}) \begin{bmatrix} C_{1}(A - B) + C_{2}(A + B) & -C_{1}(A - B) + C_{2}(A + B) \\ -C_{1}(A - B) + C_{2}(A + B) & C_{1}(A - B) + C_{2}(A + B) \end{bmatrix}$$

$$= (\frac{1}{2}) \begin{bmatrix} (A - B)^{-1}(A - B) + (A + B)^{-1}(A + B) & -(A - B)^{-1}(A - B) + (A + B)^{-1}(A + B) \\ -(A - B)^{-1}(A - B) + (A + B)^{-1}(A + B) & (A - B)^{-1}(A - B) + (A + B)^{-1}(A + B) \end{bmatrix}$$

$$=(\frac{1}{2})\left[\begin{array}{cc}I+I&-I+I\\-I+I&I+I\end{array}\right]=(\frac{1}{2})\left[\begin{array}{cc}2I&0\\0&2I\end{array}\right]=\left[\begin{array}{cc}I&0\\0&I\end{array}\right]=[I]$$

Also, Eq. (8) is proved by performing a similar matrix operation as shown in Eq. (9) and summarized in Eq. (10).

$$[K_{1}]^{-1}[K_{1}] = \begin{bmatrix} D_{1} & D_{2} \\ D_{2} & D_{1} \end{bmatrix} \begin{bmatrix} A & B \\ B & A \end{bmatrix}$$

$$= \begin{bmatrix} D_{1}A + D_{2}B & D_{1}B + D_{2}A \\ D_{2}A + D_{1}B & D_{2}B + D_{1}A \end{bmatrix} \quad (10)$$

$$= \begin{bmatrix} I & 0 \\ 0 & I \end{bmatrix}$$

$$= [I]$$

Eqs. (2) to (6) demonstrate that for inverse calculation of a matrix in the form  $\mathbf{K}_1$  with dimensions  $2n \times 2n$ , it is sufficient that two matrices (the matrices  $\mathbf{C}_1$  and  $\mathbf{C}_2$ ) with dimensions  $n \times n$ , which are half the dimensions of the main matrix, are inverted.

### 2.2. Theorem 2

Suppose that the matrix  $\mathbf{K}_2$  is in the form of Eq. (11).

$$[K_{2}] = \begin{bmatrix} [A]_{n \times n} & [0]_{n \times n} & [Q]_{n \times k} \\ [0]_{n \times n} & [A]_{n \times n} & [Q']_{n \times k} \\ [Q]_{k \times n}^{\mathrm{T}} & [Q']_{k \times n}^{\mathrm{T}} & [X]_{k \times k} \end{bmatrix}_{(2n+k) \times (2n+k)}$$

$$(11)$$

where n and k are the dimensions of the matrices  $\mathbf{A}$  and  $\mathbf{X}$ , respectively. Provided that the matrices  $\mathbf{A}$  and  $X - Q^T C_1 Q - Q'^T C_1 Q'$  are invertible, the inverse of the matrix  $\mathbf{K}_2$  is obtained from Eq. (12).

$$[K_{2}]^{-1} = \begin{bmatrix} [D_{11}]_{n \times n} & [D_{12}]_{n \times n} & [D_{13}]_{n \times k} \\ [D_{12}]_{k \times n}^{\mathrm{T}} & [D_{22}]_{n \times n} & [D_{21}]_{n \times k} \\ [D_{13}]_{k \times n}^{\mathrm{T}} & [D_{21}]_{k \times n}^{\mathrm{T}} & [D_{33}]_{k \times k} \end{bmatrix}_{(2n+k) \times (2n+k)}$$

$$(12)$$

$$[K_{2}][K_{2}]^{-1} = \begin{bmatrix} A & 0 & Q \\ 0 & A & Q' \\ Q^{T} & Q'^{T} & X \end{bmatrix} \begin{bmatrix} D_{11} & D_{12} & D_{13} \\ D_{12}^{T} & D_{22} & D_{23} \\ D_{13}^{T} & D_{23}^{T} & D_{33} \end{bmatrix}$$

$$[1ex] = \begin{bmatrix} AD_{11} + QD_{13}^{T} & AD_{12} + QD_{23}^{T} & AD_{13} + QD_{33} \\ AD_{12}^{T} + Q'D_{13}^{T} & AD_{22} + Q'D_{23}^{T} & AD_{23} + Q'D_{33} \\ Q^{T}D_{11} + Q'^{T}D_{12}^{T} + XD_{13}^{T} & Q^{T}D_{12} + Q'^{T}D_{22} + XD_{23}^{T} & Q^{T}D_{13} + Q'^{T}D_{23} + XD_{33} \end{bmatrix}$$

$$= \begin{bmatrix} I & 0 & 0 \\ 0 & I & 0 \\ 0 & 0 & I \end{bmatrix} = [I]$$

$$(23)$$

In addition, Eq. (22) is also proved similar to the given in Eq. (24). previous process, and a summary of the calculations is

$$[K_2]^{-1}[K_2] = \begin{bmatrix} D_{11} & D_{12} & D_{13} \\ D_{12}^{\mathrm{T}} & D_{22} & D_{21} \\ D_{13}^{\mathrm{T}} & D_{21}^{\mathrm{T}} & D_{33} \end{bmatrix} \begin{bmatrix} A & 0 & Q \\ 0 & A & Q' \\ Q^{\mathrm{T}} & Q'^{\mathrm{T}} & X \end{bmatrix} = \begin{bmatrix} I & 0 & 0 \\ 0 & I & 0 \\ 0 & 0 & I \end{bmatrix} = [I]$$

$$(24)$$

First, the matrices  $C_1$  and  $C_2$  are calculated from Eqs. (13) and (14), respectively. Then, the matrices  $D_{11}$ ,  $D_{22}$ ,  $D_{33}$ ,  $D_{12}$ ,  $D_{13}$ , and  $D_{23}$  are calculated according to Eqs. (15) to (20), respectively.

$$C_1 = (A)^{-1} (13)$$

$$C_2 = (X - Q^T C_1 Q - Q'^T C_1 Q')^{-1}$$
 (14)

$$D_{11} = C_1 + C_1 Q C_2 Q^T C_1 (15)$$

$$D_{22} = C_1 + C_1 Q' C_2 Q'^T C_1 (16)$$

$$D_{33} = C_2 (17)$$

$$D_{12} = C_1 Q C_2 Q'^T C_1 (18)$$

$$D_{13} = -C_1 Q C_2 (19)$$

$$D_{23} = -C_1 Q' C_2 (20)$$

Proof of Theorem 2: By considering the uniqueness of the matrix inverse, Eqs. (21) and (22) must be proved.

$$[K_2][K_2]^{-1} = [I]$$
 (21)

$$[K_2]^{-1}[K_2] = [I]$$
 (22)

This theorem can be proved using Eq. (23) by substituting six matrices  $\mathbf{D}_{11}$ ,  $\mathbf{D}_{22}$ ,  $\mathbf{D}_{33}$ ,  $\mathbf{D}_{12}$ ,  $\mathbf{D}_{13}$ , and  $\mathbf{D}_{23}$  from Eqs. (15) to (20) and performing algebraic operations and simplification. The calculation details are not disclosed in Eq. (23) due to the similarity with the proof of Theorem 1 and the avoidance of lengthening.

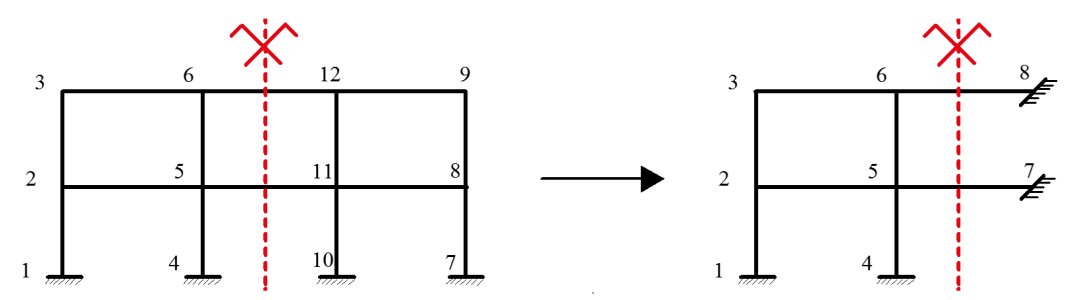


Fig. 1. Numbering of the nodes in a symmetrical skeletal structures from  $S_1$  group.

According to Eq. (12) to Eq. (20), the inverse of the matrix  $\mathbf{K}_2$  with dimensions  $(2n+k)\times(2n+k)$  can be derived by inverse calculation of two matrices with dimensions smaller than the main matrix.

One of these two matrices has dimensions  $n \times n$  (matrix  $\mathbf{C}_1$ ), and the other has dimensions  $k \times k$  (matrix  $\mathbf{C}_2$ ).

### 3. The Proposed Approach for Optimal Analysis of Symmetric Skeletal Structures

This section presents a systematic, programmable, and step-by-step approach for analyzing symmetric structures. It is important to note that the structure's symmetry is not determined solely by its geometrical symmetry. Support conditions, material's physical properties, and member's cross-sections must all be symmetrical at the same time for a structure to be considered symmetrical. In this study, symmetrical structures are divided into two general groups, which are called the  $S_1$  group and the  $S_2$  group. The structure whose axis of symmetry does not pass through any node and intersects only the structure members is defined as a symmetric structure from the  $S_1$  group. However, in a symmetrical structure from the  $S_2$  group, the axis of symmetry passes through the nodes of the structure. After determining the structure's symmetric group, a step-by-step approach is presented for that group.

## 3.1. Step-by-step Approach for Analysis of Symmetrical Skeletal Structures From the $S_1$ Group

For the analysis of symmetric structures from the  $S_1$  group, the nodes of the structure must be numbered appropriately. First, the nodes of the left half of the structure are numbered arbitrarily. The nodes of the right half are then numbered in the same order as the nodes of the left half. The difference between the numbers of the two corresponding nodes on the right and left sides of the structure must be a constant value for all nodes in this numbering. Fig. 1 shows an example of this numbering for a symmetric frame from the  $S_1$  group.

The structural stiffness matrix is obtained using this numbering method, as shown in Eq. (25).

$$\bar{K}_1 = \left[ \begin{array}{cc} A & \bar{B} \\ \bar{B}^{\mathrm{T}} & \bar{A} \end{array} \right] \tag{25}$$

6The structural stiffness matrix can be converted into the matrix  $\mathbf{K}_1$  using Eq. (26), and its inverse can be calculated using Eqs. (2) to (6).

$$\begin{bmatrix} I & 0 \\ 0 & T \end{bmatrix} \begin{bmatrix} \bar{K}_1 \end{bmatrix} \begin{bmatrix} I & 0 \\ 0 & T \end{bmatrix} = \begin{bmatrix} I & 0 \\ 0 & T \end{bmatrix} \begin{bmatrix} A & \bar{B} \\ \bar{B}^T & \bar{A} \end{bmatrix} \begin{bmatrix} I & 0 \\ 0 & T \end{bmatrix}$$
$$= \begin{bmatrix} ccA & B \\ B & A \end{bmatrix} = K_1$$
(26)

where  $\mathbf{T}$  is a matrix with the same dimensions as matrix  $\mathbf{A}$  and is computed using Eq. (27).

$$T = \begin{bmatrix} \bar{T} & & & \\ & \bar{T} & & \\ & & \cdot & \\ & & & \cdot \\ & & & \bar{T} \end{bmatrix}$$
 (27)

where  $\bar{T}$  is a matrix derived from Eq. (28), depending on the type of structure (truss or frame).

$$\begin{cases}
\bar{T} = \begin{bmatrix} 1 & 0 & 0 \\ 0 & -1 & 0 \\ 0 & 0 & 1 \end{bmatrix} & \text{for plannar frame} \\
\bar{T} = \begin{bmatrix} -1 & 0 \\ 0 & 1 \end{bmatrix} & \text{for plannar truss}
\end{cases} \tag{28}$$

By having the inverse of the matrix  $\mathbf{K}_1$ , it is possible to obtain the inverse of the matrix  $\bar{K}_1$ , which is the purpose of structural analysis, according to Eq. (29).

$$\begin{bmatrix} \bar{K}_1 \end{bmatrix}^{-1} = \begin{bmatrix} I & 0 \\ 0 & T \end{bmatrix} \begin{bmatrix} K_1 \end{bmatrix}^{-1} \begin{bmatrix} I & 0 \\ 0 & T \end{bmatrix}$$
 (29)

Meanwhile, it can be seen from Eq. (26), that the matrices **B** and  $\bar{B}$  have a relationship according to Eq. (30).

$$B = \bar{B}T \tag{30}$$

These equations demonstrate that only the matrices  $\mathbf{A}$  and  $\mathbf{B}$  are required for the formation of the matrix  $\mathbf{K}_1$  to analyze symmetric structures from the  $S_1$  group. These matrices are obtained using half of the

structure and without forming and assembling the stiffness matrix of all structure members. As a result, the following step-by-step approach for the analysis of symmetric structures from the  $S_1$  group can be presented:

Step 1- First, the nodes of the structure are numbered according to the described method.

Step 2- The main structure is halved, and the halved structure's stiffness matrix is created. Then, the matrices  $\bf A$  and  $\bar{B}$  from inside of this stiffness matrix are extracted. As shown in Fig. 1, in the halved structure, all members that intersect the symmetry axis of the structure must be present.

Step 3- The matrix  $\mathbf{T}$  is produced according to Eq. (27), depending on the type of structure (planar truss or planar frame) and the dimensions of the matrix  $\mathbf{A}$ . Then matrix  $\mathbf{B}$  is calculated using Eq. (30).

Step 4- By having the matrices  $\mathbf{A}$  and  $\mathbf{B}$  and using Eqs. (3) to (6), the matrices  $\mathbf{D}_1$  and  $\mathbf{D}_2$  are obtained.

Step 5- By obtaining the matrices  $\mathbf{D}_1$ ,  $\mathbf{D}_2$ , and  $\mathbf{T}$ , the inverse of the main structure's stiffness matrix is derived according to Eq. (31). Also, displacements of the structure are calculated using Eq. (32).

$$\begin{bmatrix} \bar{K}_1 \end{bmatrix}^{-1} = \begin{bmatrix} D_1 & D_2 T \\ T D_2 & T D_1 T \end{bmatrix}$$
 (31)

$$\{\Delta\} = \left[\bar{K}_1\right]^{-1} \{F\} \tag{32}$$

Eq. (32) identifies  $\Delta$  as the vector of node displacements, and **F** as the vector of external loads.

Step 6 - The internal forces (axial force, flexural moment, and shear force) of all members can be determined after the nodal displacements have been calculated.

Step 7- By calculating the internal forces of members, normal and shear stresses can be derived and used to evaluate the constraints of the optimization problem.

# 3.2. Step-by-step Approach for Analysis of Symmetrical Skeletal Structures From the $S_2$ Group

Proper numbering of nodes in the analysis of symmetric structures from the  $S_2$  group must also be consid-

ered. First, arbitrary numbering is done for the left-half nodes. Then, the right-half nodes are numbered in the same order. It is necessary to mention that according to Fig. 2, the difference in the node number between the two corresponding nodes in the right and left halves of the structure must be a constant number for all nodes. Finally, the nodes at the intersection of the symmetry axis are numbered.

The structural stiffness matrix is obtained using this numbering method, as shown in Eq. (33).

$$\bar{K}_2 = \begin{bmatrix} A & 0 & Q \\ 0 & \bar{A} & \bar{Q} \\ Q^{\mathrm{T}} & \bar{Q}^{\mathrm{T}} & X \end{bmatrix}$$
(33)

When the matrix  $\bar{K}_2$  is converted to  $\mathbf{K}_2$  using Eq. (34), the inverse of the structure's stiffness matrix can be calculated using Eqs. (12) to (20).

$$\begin{bmatrix} I & 0 & 0 \\ 0 & T & 0 \\ 0 & 0 & I \end{bmatrix} \begin{bmatrix} \bar{K}_2 \end{bmatrix} \begin{bmatrix} I & 0 & 0 \\ 0 & T & 0 \\ 0 & 0 & I \end{bmatrix} = \begin{bmatrix} I & 0 & 0 \\ 0 & 0 & I \end{bmatrix} = \begin{bmatrix} I & 0 & 0 \\ 0 & \bar{A} & \bar{Q} \\ Q^T & \bar{Q}^T & X \end{bmatrix} \begin{bmatrix} I & 0 & 0 \\ 0 & T & 0 \\ 0 & 0 & I \end{bmatrix} = (34)$$

$$\begin{bmatrix} A & 0 & Q \\ 0 & A & Q' \\ Q^T & Q'^T & X \end{bmatrix} = K_2$$

Eqs. (27) and (28) are used to produce the matrix **T** in Eq. (34) using the same procedure as in Section 3.1.

$$[\bar{K}_2]^{-1} = \begin{bmatrix} I & 0 & 0 \\ 0 & T & 0 \\ 0 & 0 & I \end{bmatrix} [K_2]^{-1} \begin{bmatrix} I & 0 & 0 \\ 0 & T & 0 \\ 0 & 0 & I \end{bmatrix}$$
 (35)

By having the matrix  $\bar{Q}$  and applying Eq. (36), the matrix Q' can also be calculated.

$$Q' = T\bar{Q} \tag{36}$$

The matrices  $\mathbf{A}$ ,  $\mathbf{X}$ ,  $\mathbf{Q}$ , and Q' are required for the analysis of symmetric structures from the  $S_2$  group.

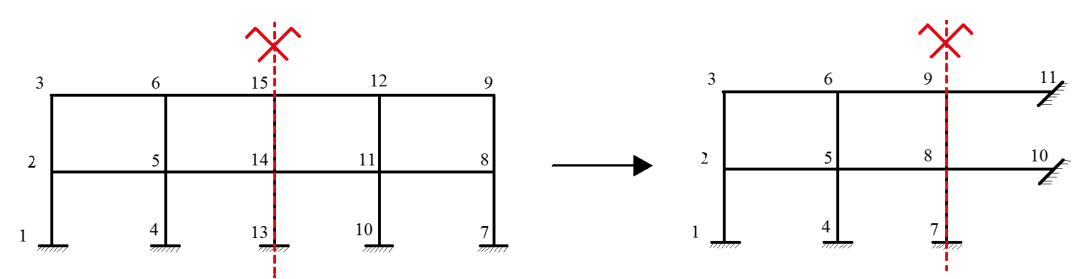


Fig. 2. Numbering of the nodes in a symmetrical skeletal structure from the S<sub>2</sub> group.

These matrices are extracted from the stiffness matrix of the halved structure by modeling half of it. Therefore, there is no need to model and calculate the stiffness matrix for the whole structure. For the analysis of symmetric structures from the S2 group, the following step-by-step approach can be used:

Step 1- Appropriate numbering for structural nodes is done according to the described method.

Step 2- The halved structure is modeled, and its stiffness matrix is formed. It is important to note that in the halved model of the structure, all members connecting to nodes along the structure's symmetry axis must be present. An example of this halving in a symmetric frame structure from the  $S_2$  group is shown in Fig. 2. The matrices  $\mathbf{A}$ ,  $\mathbf{X}$ ,  $\mathbf{Q}$ , and  $\bar{Q}$  are then computed using the stiffness matrix of the halved structure.

Step 3- By creating a matrix **T** from Eq. (27) with dimensions equal to the matrix **A** and considering the type of structure, the matrix Q'can be obtained using Eq. (36).

Step 4- By calculating the matrix Q' from Step 3 and the matrices  $\mathbf{A}$ ,  $\mathbf{X}$ , and,  $\mathbf{Q}$  from Step 2, the submatrices  $\mathbf{D}_{11}$ ,  $\mathbf{D}_{22}$ ,  $\mathbf{D}_{33}$ ,  $\mathbf{D}_{12}$ ,  $\mathbf{D}_{13}$ , and  $\mathbf{D}_{23}$  can be

calculated from Eqs. (15) to (20), respectively.

Step 5 - From the submatrices calculated in Step 4, the stiffness matrix of the main structure and its displacements are computed using Eqs. (37) and (38).

$$\begin{bmatrix} \bar{K}_2 \end{bmatrix}^{-1} = \begin{bmatrix} D_{11} & D_{12}T & D_{13} \\ TD_{12}^{\mathrm{T}} & TD_{22}T & TD_{23} \\ D_{13}^{\mathrm{T}} & D_{23}^{\mathrm{T}}T & D_{33} \end{bmatrix}$$
(37)

$$\{\Delta\} = \left[\bar{K}_2\right]^{-1} \{F\} \tag{38}$$

In the symmetry structures from the  $S_2$  group, Steps 6 and 7 are similar to those from the  $S_1$  group. The proposed approach for analysis of symmetric structures from the  $S_1$  groups and  $S_2$  groups is shown in Fig. 3.

### 4. Formulation of RBDO Problem

### $\begin{array}{cccc} \textbf{4.1.} & Reliability\text{-}Based & Design & Optimization \\ & Method & \end{array}$

The general form of a Reliability-Based Design Optimization (RBDO) can be represented as Eq. (39),

Find: 
$$d, \mu_X$$
 to minimize:  $f(d, X, P)$  subject to: 
$$\begin{cases} \text{Deterministic constraint: } g_i(d, X, P) \leq 0 & i = 1, 2, ..., m \\ \text{Probabilistic constraint: } (P_s)_j = \text{Prob}\left(\bar{g}_j(d, X, P) \leq 0\right) \geq (P_s^{\text{target}})_j & j = 1, 2, ..., n \\ d^{\text{L}} \leq d \leq d^{\text{U}} &, \quad \mu_X^{\text{L}} \leq \mu_X \leq \mu_X^{\text{U}} \end{cases}$$
(39)

where **d** denotes the vector of deterministic design variables. Furthermore,  $\mu_X$  and  $\mu_P$  are the mean vectors of random variables **X** and random parameters **P**, respectively. In size optimization problems, f is usually the structure's weight. Also,  $g_i$  is the  $i^{th}$  deterministic constraint. In addition,  $\mathbf{d}^L$ ,  $\mathbf{d}^U$ ,  $\mu_X^L$ , and  $\mu_X^U$  are called the lower and upper bounds of **d** and **X**, respectively.  $(P_s^{target})_j$ ,  $(P_s)_j$ , and  $\bar{g}_j$  indicate the target probability of safety, probability of safety, and limit state function related to the  $j^{th}$  probabilistic constraint, respectively. The probability of satisfying  $\bar{g}_j$  (**d**, **X**, **P**)  $\leq 0$  for the  $j^{th}$  limit state function is represented by Prob ( $\bar{g}_j$  (**d**, **X**, **P**)  $\leq 0$ ).

Besides, m and n denote the number of deterministic and probabilistic constraints, in turn.

### 4.2. Enhanced Vibrating Particle System (EVPS)

The RBDO problem is solved using an expanded vibrating particle system (EVPS) method in this study. This algorithm has been used to solve various engineering optimization problems [34-40]. The vibrating particles system (VPS) method was developed by Kaveh

and Ilchi [41] and is according to the free vibration of single-degree-of-freedom systems with viscous dampening. The EVPS was then proposed by Kaveh et al. [42] to modify and improve the VPS' efficiency. By applying these modifications, the convergence speed is increased. Also, the EVPS' search capability has been enhanced, allowing it to avoid local optimal solutions. Eventually, all of this leads to better results. One distinction between VPS and EVPS is that the parameter of historically best position within the entire population (HB) of the VPS algorithm is replaced with a memory parameter in the EVPS, which holds the number of memory sizes of the best historic locations in the entire population. If each iteration's best solution is better than the worst solution from the previous iteration, the best solution from each iteration should replace the previous iteration's worst value in memory. In addition, the population generation equations are changed for the next iteration in the EVPS. In EVPS, for each particle, there are three different weights. The particles move closer to equilibrium positions via adjusting these weights. Diversification and intensification are also brought into balance.

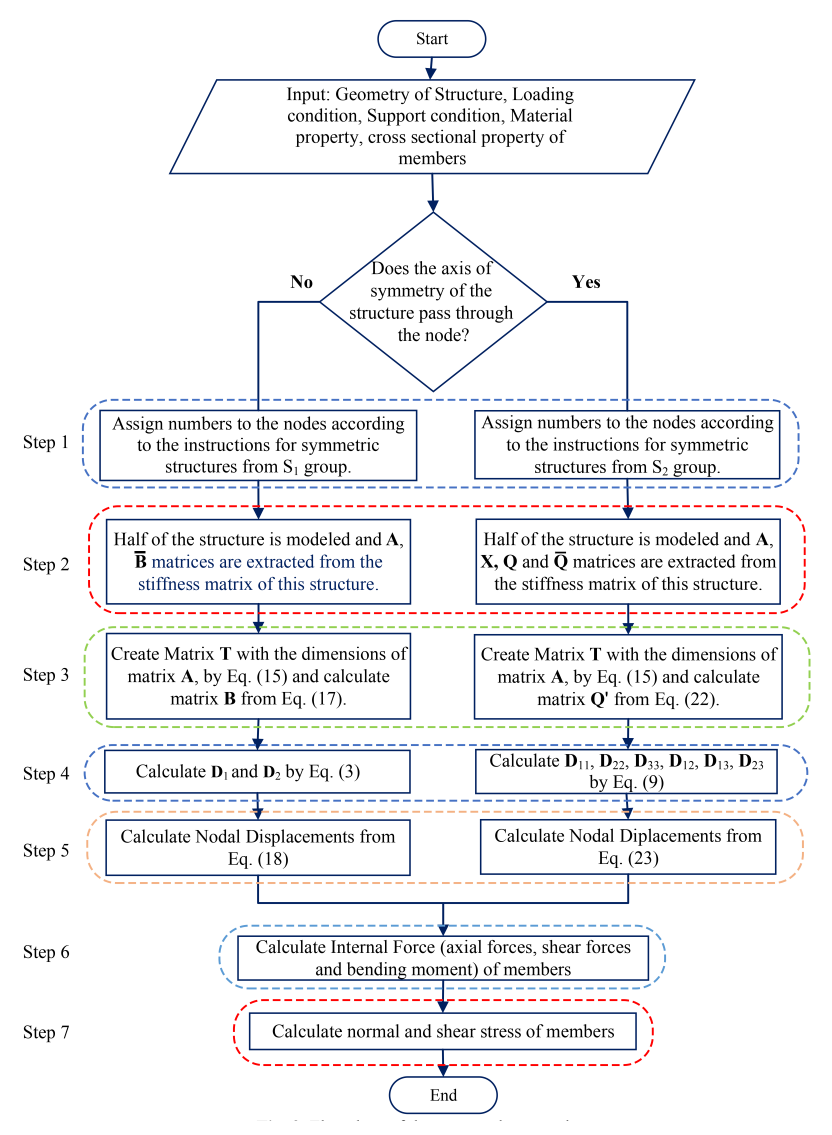


Fig. 3. Flowchart of the proposed approach.

### 5. Illustrative Example

This problem compares the efficiency of the proposed approach for symmetrical frames with different numbers of bays and stories. To compare the proposed approach with the direct approach, which does not use the structure's symmetry properties, frame structures were analyzed. Fig. 4 shows the geometry In this study, the average time of of this frame. structural analysis by direct methods and the proposed approach for frames of the S<sub>1</sub> and S<sub>2</sub> groups with a different number of bays and stories were investigated. For symmetrical frames of the  $S_1$  group, 5, 11, and 21 bays were considered, and for symmetrical frames of the  $S_2$  group, 4, 10, and 20 bays were considered. The Young's modulus, cross-sectional area, and moment of inertia of the members are equal to  $2.1 \times 10^{11} \text{N/m}^2$  ( $3.05 \times 10^4 \text{ ksi}$ ),  $47.8 \times 10^{-4} \text{ m}^2$  $(7.41in^2)$ , and  $14.84 \times 10^{-8} \text{m}^4$   $(0.357 in^4)$ , respectively. Grouping of these frames based on the number of bays

and analysis method is provided in Table 1.

Figs. 5 and 6 display the computational time for the frames from the  $S_1$  and  $S_2$  groups, respectively. All problems are coded in MATLAB software using the finite element method. The structural analysis was performed in Windows 10 (64-bit operating system) with an Intel (R) Core (TM) i7-7700HQ CPU @ 2.80 GHz processor and a 32 GB installed RAM. According to the results, the difference in computational time between the direct method and the proposed approach in frame analysis is related to the number of bays and stories in the frames. So that with increasing the number of bays and stories, the computational time difference between the proposed approach and direct analysis increases and vice versa. This is due to the fact that as the number of bays and stories increases, the problem gets larger in dimensions. Thus, the proposed approach removes more degrees of freedom and members by modeling half of the structure.

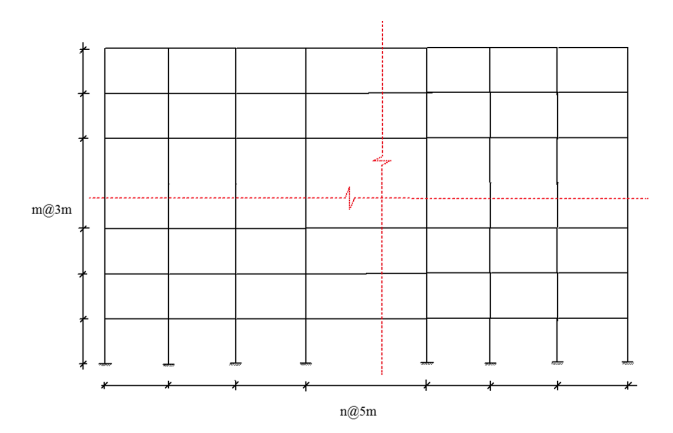


**Fig. 4.** Symmetric frame structure with n spans and m stories.

Table 1
Frame structure group.

	1	
Name of group	Number of bays	Method of analysis
5B-D	5	Direct method
5B-P	5	Proposed approach
11B-D	11	Direct method
11B-P	11	Proposed approach
21B-D	21	Direct method
21B-P	21	Proposed approach
4B-D	4	Direct method
4B-P	4	Proposed approach
10B-D	10	Direct method
10B-P	10	Proposed approach
20B-D	20	Direct method
20B-P	20	Proposed approach

As shown in Figs. 5 and 6, it is evident that for a certain number of bays and with an increasing number of stories, the time difference between the proposed approach and the direct method increases. When the number of stories remains constant but the number of bays increases, the difference becomes even more significant. The cause of the issue is that when the number of stories remains constant but the number of bays increases, halving the structure removes a considerable number of members and degrees of freedom. The time required to create and assemble the structural stiffness matrix decreases as the number of members decreases. The dimensions of the matrices required for structural analysis and the computational time to inverse them decrease as the degrees of freedom decrease.

### 6. Numerical Problems

Two standard structures are studied in this section to exhibit the effectiveness of this approach in comparison to the direct method. In this study, symmetrical structures are divided into two general groups, which are called the  $S_1$  group and the  $S_2$  group. The structure whose axis of symmetry does not pass through

any node and intersects only the structure members is defined as a symmetric structure from the  $S_1$  group. However, in a symmetrical structure from the  $S_2$  group, the axis of symmetry passes through the nodes of the structure. In the first example, the structure is from the  $S_1$  group and in the second example, the structure is from the  $S_2$  group. The purpose of this study is to optimize the size of two structures that have random variables and probabilistic constraints. These structures are:

- A 3-bay 15-story frame
- A 200-bar planar truss

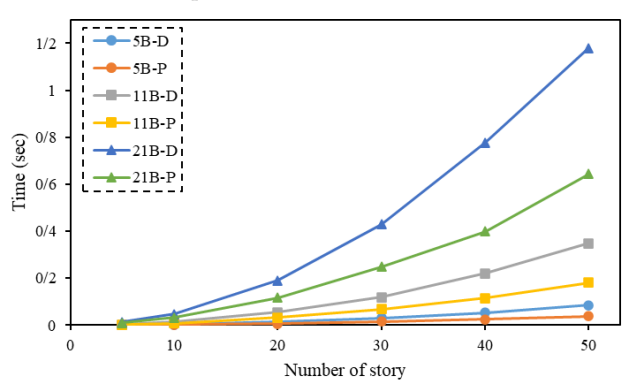


**Fig. 5.** Computational time for analysis of frame structure from  $S_1$  group.

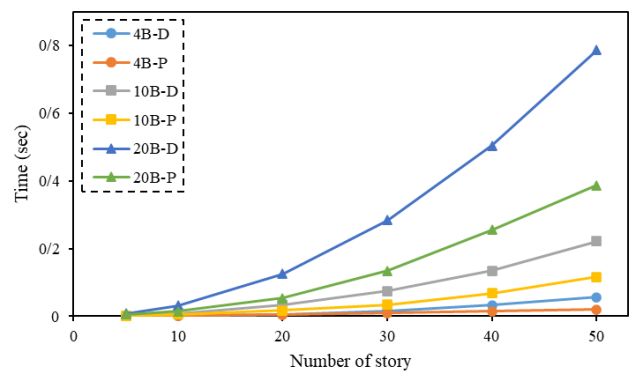


**Fig. 6.** Computational time for analysis of frame structure from  $S_2$  group.

The EVPS in the RBDO problem has a population size of 30 and a maximum number of iterations of 300. The reliability of constraints in the inner loop of the RBDO problem was evaluated using the MCS method with  $10^5$  samples. Each problem is solved in 10 independent runs to ensure the EVPS performance. The first problem is the symmetric structure from the  $S_1$  group, and the second problem is the symmetric structure from the  $S_2$  group.

### 6.1. A 3-bay 15-story Frame

A 15-story frame with three bays is illustrated in Fig. 7, which shows the geometry, loading, grouping of members, and numbering of its nodes. This frame is

symmetrical due to the symmetry in the geometry, the support conditions, the mechanical properties of the materials, and the geometric characteristics of members' cross-sections. The frame's axis of symmetry does not intersect any nodes. Therefore, this structure is in the S<sub>1</sub> group of symmetrical structures. This frame, which is a well-known benchmark problem, has been investigated by many researchers [43, 44]. This frame has 64 nodes and 105 members. The frame members are organized into ten groups of columns and one group of beams (11 groups in total). The number of random variables in this problem is 11, the number of random parameters is 3, and there are 14 statistical variables in total. The cross-section of members of this frame is a random design variable of the problem, and concentrated lateral load, distributed gravity load of beams, and modulus of elasticity of steel materials of the frame are random parameters of the problem. Table 2 shows the statistical characteristics of these variables. The problem's random design variables are selected discretely from 267 W-sections. The yield stress  $(F_y)$  and weight per volume  $(\gamma)$  for the materials of this frame are 248.2 MPa (36ksi) and  $76.819 \text{kN/m}^3$  (0.283lb/in<sup>3</sup>), respectively. The effective length factors in all members are assumed to be  $k_x \ge 1.0$  for in-plane buckling and  $k_y = 1.0$  for out-of-plane buckling. Also, it is assumed that all columns are non-braced along their length, and all beams have a non-braced length equal to one-fifth of the span length.

 $\begin{tabular}{ll} \textbf{Table 2} \\ \textbf{Statistical characteristics of variables for the 3-bay 15-story} \\ \textbf{frame.} \\ \end{tabular}$ 

Variable	Distribution	Mean	$\overline{\text{CV}}$
$\overline{A_i}$	Normal	Design Varabile	0.05
P, kN (kips)	Normal	30 (6.75) 0.10	
W, kN/m (kips/ft)	Normal	50 (3.42)	0.10
E, GPa (ksi)	Normal	200 (29000)	0.05

The problem's constraints are based on design limitations for steel moment-resisting frames according to the AISC-LRFD [45]. The problem's probabilistic constraint is related to the structure's roof drift and is derived from Eq. (40).

$$P_s = \operatorname{Prob}\left(\frac{|\Delta_T|}{H} - R \le 0\right) \ge P_s^{\text{target}} = 99.865\%$$
(40)

where  $\Delta_T$ , H, and R are the roof drift, height of the frame, and maximum drift index, respectively. In this study, the value of R is considered to be  $\frac{1}{300}$ . The problem also has two deterministic constraints. Eq. (41) provides the first deterministic constraint, which is associated with the inter-story drift.

$$\frac{|d_i|}{h_i} - R_l \le 0 \quad i = 1, 2, ..., n_s \tag{41}$$

where  $h_i$ ,  $d_i$ ,  $n_s$ , and  $R_l$  are the  $i^{th}$  floor's story height, the  $i^{th}$  floor's inter-story drift, the total number of stories, and the index of inter-story drift, respectively.

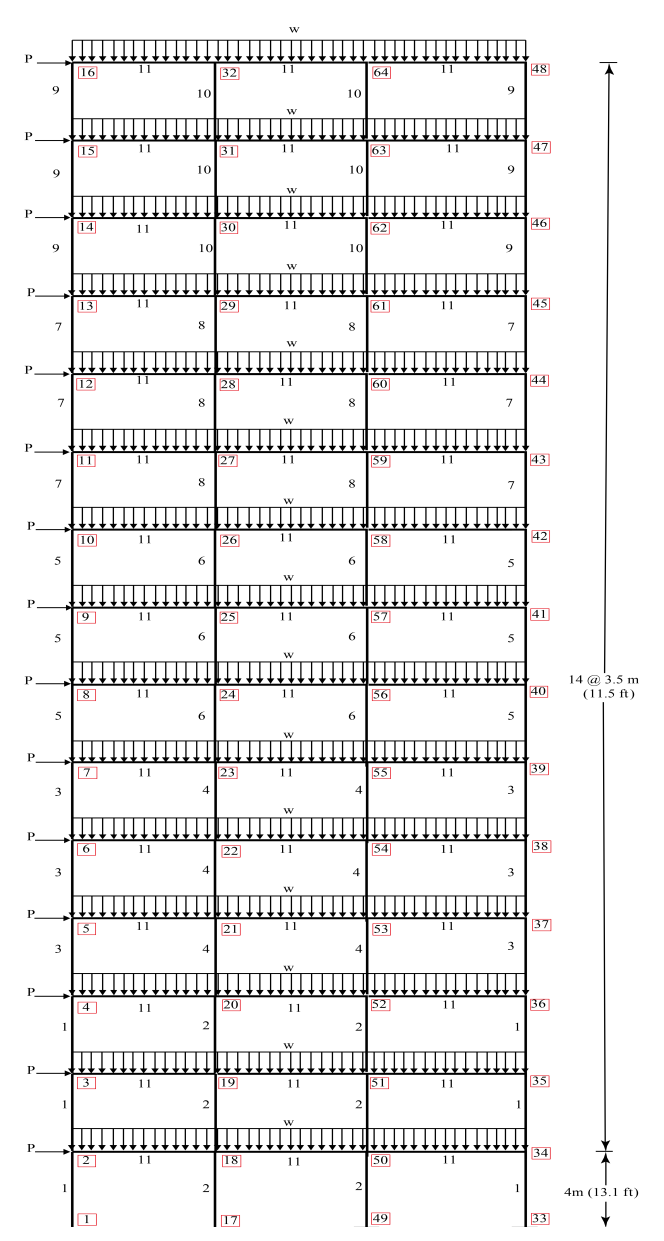


Fig. 7. A 3-bay 15-story frame.

The value of  $R_l$  in this problem is equal to  $\frac{1}{300}$ . The second deterministic constraint is also about the strength of the frame members and is obtained from Eq. (42).

$$\frac{p_u}{2\phi_c p_n} + \left[\frac{M_{ux}}{\phi_b M_{nx}} + \frac{M_{uy}}{\phi_b M_{ny}}\right] - 1 \le 0 \quad \text{for } \frac{p_u}{\phi_c p_n} \le 0.2$$

$$\frac{p_u}{\phi_c p_n} + \frac{8}{9} \left[\frac{M_{ux}}{\phi_b M_{nx}} + \frac{M_{uy}}{\phi_b M_{ny}}\right] - 1 \le 0 \quad \text{for } \frac{p_u}{\phi_c p_n} \ge 0.2$$

$$(42)$$

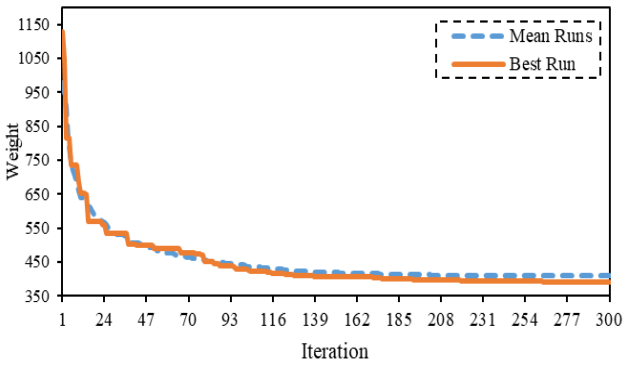
where  $M_u$  and  $P_u$  indicate the required bending and axial strength, respectively. These values will be determined by the structural analysis.  $M_n$  and  $P_n$  are the nominal bending and axial strength for the tension and

compression members, respectively. These parameters will be calculated from the load and resistance factor design (LRFD) [45]. Furthermore,  $\phi_c$  represents the axial resistance reduction factor, It is 0.90 for tension members and 0.85 for compression members. Also,  $\phi_b$  is equal to 0.90, which is the bending resistance reduction factor.

The optimal design, and the best, worst, mean, and standard deviation of the weight calculated by the EVPS are all provided in Table 3. Fig. 8 illustrates the EVPS convergence plot for the best and mean runs. In addition, Figs. 9 and 10 show the stress ratio and interstory drift for the EVPS' best solution, respectively.

Table 3 Optimum designs for the 3-bay 15-story frame.

	*
	Optimal W-Shaped
	section
Members group	EVPS
1	W14X99
2	W27X161
3	W12X79
4	W27X114
5	W21X68
6	W18X86
7	W10X45
8	W21X68
9	W12X30
10	W16X40
11	W21X44
Best weight, kN (lb.)	391.88(88102.0 lb.)
Mean weight, kN (lb.)	409.11(91977.1 lb.)
Worst weight, kN (lb.)	443.67(99745.3 lb.)
Standard deviation, kN (lb.)	19.40(4361.8 lb.)
$\beta$ (Probability of safety %)	3.035~(99.88%)
in best solution	



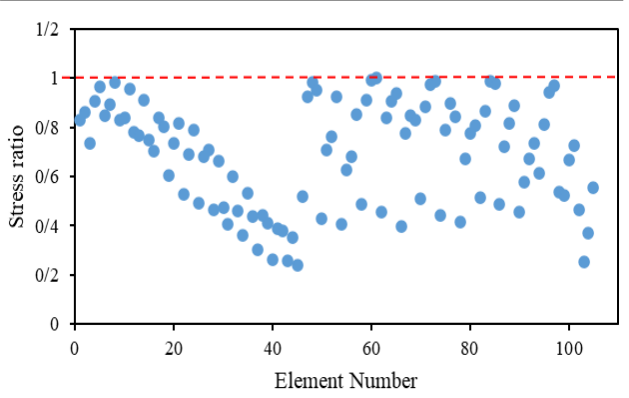
**Fig. 8.** Convergence plot for the optimal and mean runs of the EVPS of the 3-bay 15-story.

Table 4 provides an evaluation of the computational time of the proposed approach with the direct method for static analysis of the 3-bay 15-story frame structure. By the direct method, it is necessary to inverse a matrix with dimensions of  $180 \times 180$  in order to perform static analysis of the 3-bay 15-story frame. While

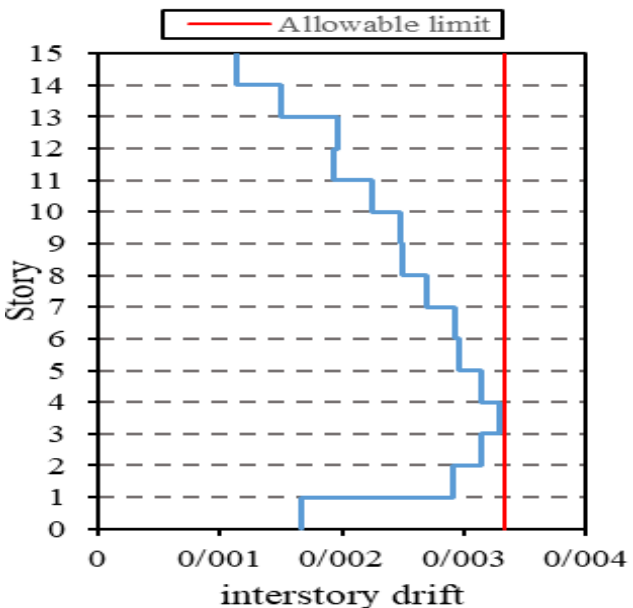
in the efficient proposed approach, two matrices with dimensions of  $90\times90$  are inverted. When the dimensions of matrices are halved, less memory is required to store the data, and it takes less time to calculate the inverse of matrices. In comparison to the direct method, the proposed approach reduces the average computational time for static analysis of the frame by 37%. The time reduction is due to the decrease in the number of members needed to assemble the stiffness matrix of the halved structure.

Table 4 Evaluation of the computational time of two methods for the 3-bay 15-story frame.

Method	Inverse	CPU time
Method	$\operatorname{problem}$	(sec)
Direct	1 matrix of	$15.416 \times 10^{-4}$
method	$180 \times 180$	15.410×10
Proposed	2 matrices of	$11.253 \times 10^{-4}$
approach	$90 \times 90$	11.255 × 10
Time ratio		1.37



**Fig. 9.** Stress ratio for the optimal design of the EVPS for the 3-bay 15-story frame.



**Fig. 10.** Inter-story drift for the optimal design of the EVPS for the 3-bay 15-story frame.

Also, it is due to the inverse calculation of matrices whose dimensions are half the dimensions of the main structure's stiffness matrix. The time it takes to find the optimal solution in EVPS is decreased by reducing the structural analysis time. So that the time required to perform 10 independent runs with a population size of 30 and a maximum iteration number of 300, using the proposed approach to analyze this frame in the optimization process, is about 60,917 minutes (1,015 hours). However, if the direct method for frame analysis is utilized in the optimization process under the same conditions, it takes about 82,846 minutes (1,380 hours). These results demonstrate the efficiency and effectiveness of the proposed approach in the repeated structural analysis that occurs when solving the RBDO problem by meta-heuristic algorithms.

### 6.2. A 200-bar Planar Truss Structure

The second problem is the 200-bar planar truss structure addressed as an example of size optimization in structural optimization research [46-48]. The geometry of this truss and the appropriate numbering for the nodes and their members are shown in Fig. 11. This truss is a symmetrical structure from the  $S_2$  group. Because, firstly, it has symmetry in geometry, support conditions, mechanical properties of materials,

and cross-sectional characteristics of members. Secondly, the truss's axis of symmetry passes through its nodes. The number of nodes of this truss is 77, the number of its members is 200, and it includes 150 degrees of freedom in total. There are 32 statistical variables, 29 random design variables, and three random parameters. Table 5 shows the statistical characteristics of these variables. The truss members are classified into 29 groups and listed in the results. The 29 random design variables for this problem were selected from the 30 sections presented in Table 6. The weight per volume of material ( $\gamma$ ) for this problem is 76.819 kN/m3 (0.283 lb/in3). The different load cases applied to this structure are listed in Table 7. This study considers the load case 3, which is a combination of cases 1 and 2.

Table 5
Statistical charactristic of variables for the 200-bar planar truss structure.

Variable	Distribution	Mean	CV
$A_i$ , cm <sup>2</sup> (in. <sup>2</sup> )	Normal	Design varabile	0.05
$P_1$ , kN (kips)	Normal	1000 (224.8)	0.10
$P_2$ , kN (kips)	Normal	10000 (2248)	0.10
E, GPa (ksi)	Normal	$3{\times}10^4\ (4.35{\times}10^6)$	0.05

Table 6
A set of 30 discrete design variables in the 200-bar planar truss structure.

Section number	$A_i$ , cm <sup>2</sup> (in. <sup>2</sup> )	Section number	$A_i$ , cm <sup>2</sup> (in. <sup>2</sup> )	Section number	$A_i$ , cm <sup>2</sup> (in. <sup>2</sup> )
1	0.64 (0.1)	11	13.81 (2.14)	21	54.99 (8.52)
2	$2.23 \ (0.34)$	12	$17.39\ (2.69)$	22	59.99 (9.3)
3	2.83 (0.44)	13	18.06 (2.8)	23	$69.99\ (10.85)$
4	3.47 (0.53)	14	20.19(3.13)	24	$85.99\ (13.33)$
5	6.15 (0.95)	15	22.99(3.56)	25	$92.19\ (14.29)$
6	6.97 (1.08)	16	24.59(3.81)	26	$110.77 \ (17.17)$
7	7.57 (1.17)	17	30.99 (4.80)	27	$123.74\ (19.18)$
8	8.59(1.33)	18	$38.39\ (5.95)$	28	$152.77 \ (23.68)$
9	9.59(1.48)	19	42.39 (6.57)	29	181.16 (28.08)
10	$11.38\ (1.76)$	20	$46.39\ (7.19)$	30	$217.41 \ (33.7)$

Table 7
Loading conditions for the 200-bar planar truss structure.

Case no.	Load kN (lb)	Direction	Nodes
1	$P_1$	X	1, 6, 15, 20, 29, 34, 43, 48, 57, 62, 71
2	$P_2$	Y	1-6, 8, 10, 12, 14-20, 22, 24, 26, 28-34, 36, 38, 40,42-48, 50, 52, 54,
			56-62, 64, 66,68, 70-75
3			Load cases 1 and 2 acting together

The problem's probabilistic constraints are related to the members' axial tension and compression stresses. These constraints are calculated from Eq. (43).

$$(P_s)_j = \operatorname{Prob}\left(\frac{|\sigma_j|}{\sigma^{\text{all}}} - 1 \le 0\right) \ge P_s^{\text{target}} = 99.865\%$$
  
for  $j = 1, 2, ..., 200$  (43)

where  $sigma_j$  and  $\sigma^{all}$  are the stress of the  $j^{th}$  member and the allowable stress of the members, respec-

tively.  $\sigma^{\rm all}$  for tension and compression members of the truss is 68.95MPa (10ksi). There are no displacement constraints in this problem, but the members' cross-sections should be greater than  $0.1 \, {\rm cm}^2$  (in.<sup>2</sup>).

Table 8 shows the results for the optimal design and the best, worst, mean, and standard deviation of the weight calculated by the EVPS and grouping of truss members. Fig. 12 shows the EVPS convergence plot for the best and mean runs. In addition, Fig. 13 shows the stress ratio for the best solution for the EVPS in this problem.

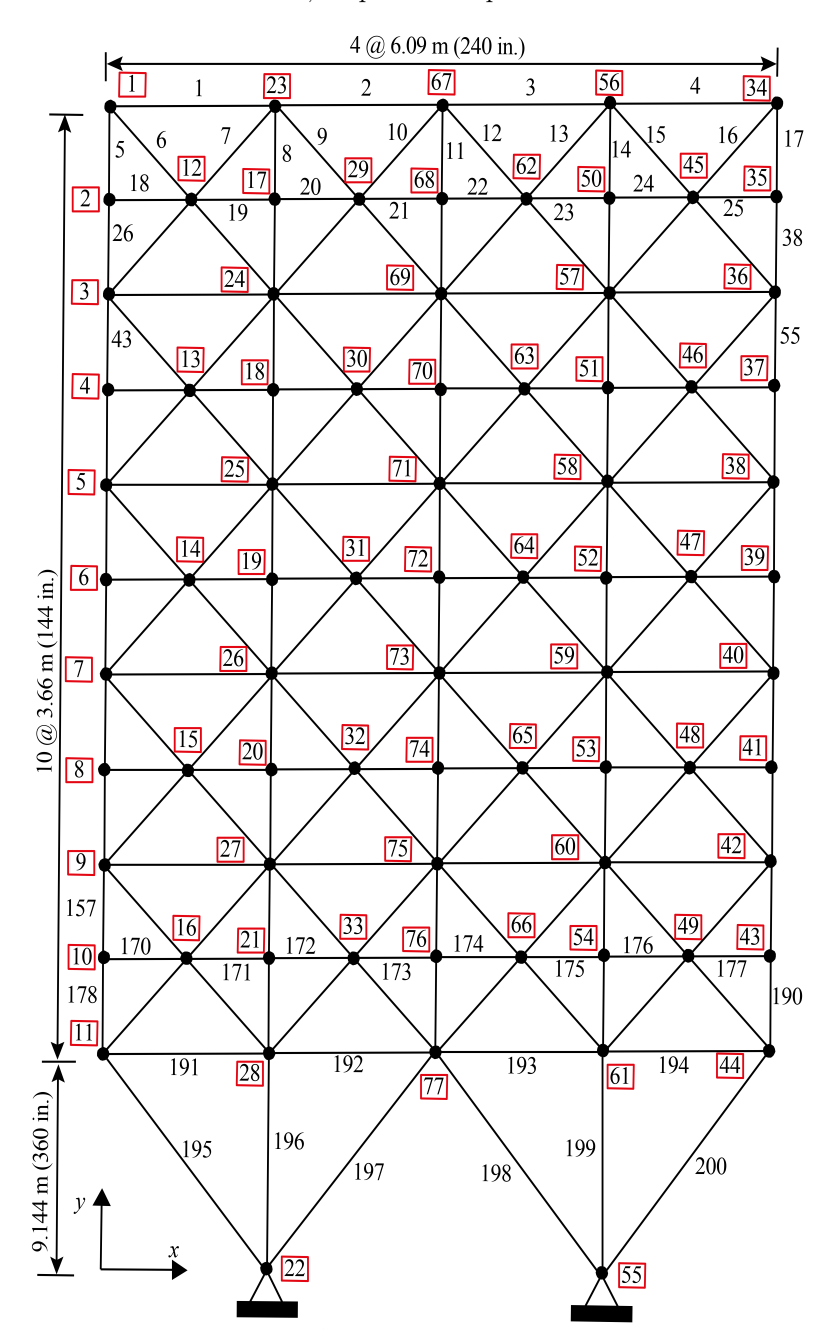
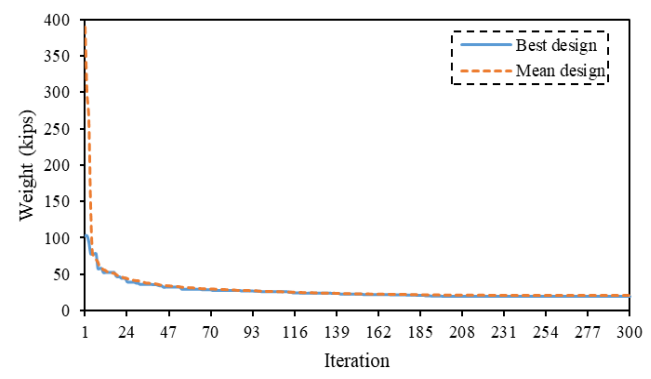
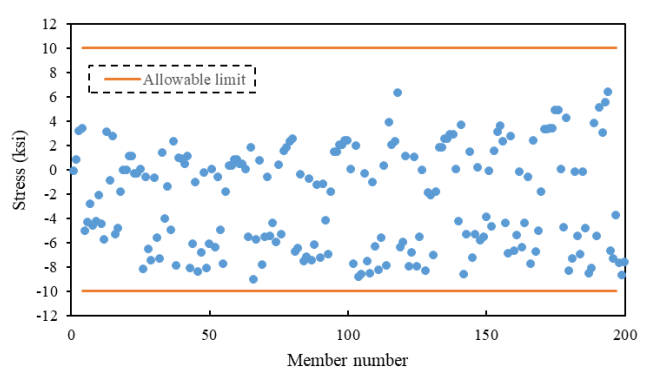


Fig. 11. A 200-bar planar truss structure.



**Fig. 12.** Convergence plot for the optimal and mean runs of the EVPS for the 200-bar planar truss structure.



**Fig. 13.** Stress constraint boundaries of the 200-bar planar truss evaluated in the optimized design by EVPS.

Table 8
Optimum designs for the 200-bar planar truss structure

Area of members group, $A_i$ , cm <sup>2</sup> (in. <sup>2</sup> )	Members in the group	EVPS
$A_1$	1, 2, 3, 4	2.23 (0.34)
$A_2$	5, 8, 11, 14, 17	$11.38\ (1.76)$
$A_3$	19, 20, 21, 22, 23, 24	$3.47 \ (0.53)$
$A_4$	18, 25, 56, 63, 94, 101, 132, 139, 170, 177	3.47(0.53)
$A_5$	26, 29, 32, 35, 38	6.97(1.08)
$A_6$	6, 7, 9, 10, 12, 13, 15, 16, 27, 28, 30, 31, 33, 34, 36, 37	2.23 (0.34)
$A_7$	39, 40, 41, 42	3.47(0.53)
$\stackrel{\cdot}{A_8}$	43, 46, 49, 52, 55	13.81(2.14)
$\stackrel{\circ}{A_9}$	57, 58, 59, 60, 61, 62	6.15 (0.95)
$A_{10}^{\circ}$	64, 67, 70, 73, 76	20.19 (3.13)
$A_{11}$	44, 45, 47, 48, 50, 51, 53, 54, 65, 66, 68, 69, 71, 72, 74, 75	$2.23 \ (0.34)$
$A_{12}$	77, 78, 79, 80	0.53(3.47)
$A_{13}$	81, 84, 87, 90, 93	22.99(3.56)
$A_{14}$	95,96, 97, 98, 99, 100	$2.83\ (0.44)^{'}$
$A_{15}$	102, 105, 108, 111, 114	20.19 (3.13)
$A_{16}$	82, 83, 85, 86, 88, 89, 91, 92, 103, 104, 106, 107, 109, 110, 112, 113	3.47 (0.53)
$A_{17}$	115, 116, 117, 118	0.64(0.10)
$A_{18}$	119, 122, 125, 128, 131	30.99 (4.80)
$A_{19}$	133, 134, 135, 136, 137, 138	$2.83 \ (0.44)^{'}$
$A_{20}$	140, 143, 146, 149, 152	46.39 (7.19)
$A_{21}$	120, 121, 123, 124, 126, 127, 129, 130, 141,142, 144, 145, 147, 148, 150, 151	3.47 (0.53)
$A_{22}$	153, 154, 155, 156	18.06(2.80)
$A_{23}$	157, 160, 163, 166, 169	$46.39\ (7.19)$
$A_{24}$	171, 172, 173, 174, 175, 176	$3.47 \ (0.53)^{'}$
$A_{25}$	178, 181, 184, 187, 190	42.39 (6.57)
$A_{26}$	158, 159, 161, 162, 164, 165, 167, 168, 179,180, 182, 183, 185, 186, 188, 189	9.59 (1.48)
$A_{27}$	191, 192, 193, 194	24.59(3.81)
$A_{28}$	195, 197, 198, 200	42.39(6.57)
$A_{29}$	196, 199	59.99 (9.30)
Best weight, kN (kips)		85.09 (19.13)
Mean weight, kN (kips)		93.27 (20.97)
Worst weight, kN (kips)		1103.91 (23.36)
Standard deviation, kN (kips)		73.66 (16.56)
Minimum of $\beta$ (Probability of safety %) in best solution		3.062 (99.89%)

Table 9 compares the computational time of the proposed approach to that of the direct method for static analysis of the 200-bar planar truss structure. The inverse calculation of a 150×150 matrix is necessary for the static analysis of the 200-bar planar truss structure. However, In the proposed approach, two matrices, one with 64×64 dimensions and the other with 22×22, must be inverted. In the proposed approach, the dimensions of the matrices to be inversed are less than half the dimensions of the main structure's stiffness matrix. Using the proposed approach, the computational time for static analysis of this truss is reduced by 98% compared to the direct method. This time savings is due to both a reduction in the number of members required to assemble the structural stiffness matrix in the halved model and a reduction in the size of the matrices that must be inversed in the proposed approach. The proposed approach also reduces the computational time required to obtain the optimal solution in the EVPS. The time required to perform 10 independent runs with a population size of 30 and a maximum iteration number of 300, using the proposed approach for analysis of this truss in the optimization process, is about 7,017 minutes (117 hours). However, if the direct method of truss analysis is employed in the optimization process with the same EVPS parameters, it takes about 13,754 minutes (229 hours). The efficiency and effectiveness of the proposed approach for the repeated analysis of the structure that occurs during the procedure of solving the RBDO problem using meta-heuristic algorithms can be proved by comparing these two times.

Table 9
Evaluation of the computational time of two methods for the 200-bar planar truss structure.

Method	Inverse	CPU time
Method	problem	(sec)
Direct method	1 matrix of $150 \times 150$	$8.998 \times 10^{-4}$
Proposed	1 matrix of $64 \times 64$	$4.454 \times 10^{-4}$
approach	and 1 matrix of 22 $\times$ 22	4.454×10
Time ratio		1.98

### 7. Conclusions

Using the properties of symmetrical structures, these structures can be analyzed more quickly and accurately. When solving problems involving large-scale structures that require many analyses, the need to reduce the analysis time of symmetrical structures becomes even more significant. Solving the RBDO problem integrated with meta-heuristic algorithms is one of these problems that require a repeated structural analysis. An efficient approach for the optimal analysis of symmetric skeletal structures is addressed in this study, and it is used to solve the RBDO problems of this type of structure. In this approach, an efficient approach for the analysis of symmetrical structures is presented,

which reduces the calculation time and the memory required for data storage. This approach, which uses a systematic and programmable process, extracts the required submatrices whose dimensions are half or less than half the dimensions of the main structure's stiffness matrix. The inverse of the main structure's stiffness matrix can then be calculated by computing the inverse of matrices with the dimensions of these submatrices and performing matrix algebra operations. In this approach, it is not necessary to create the main structure's stiffness matrix by assembling all of the stiffness matrices for each member; it is possible to analyze the main structure by creating a stiffness matrix for half of it and extracting the relevant submatrices. In the proposed approach, only one structure is modeled, and there is no need to convert the load and combine the obtained responses. However, in the conventional method for symmetrical structure analysis, two halved substructures with distinct support and loading conditions are analyzed. A symmetrical structure with general loads is turned into two structures with symmetric and antisymmetric loads using the superposition principle. Then, depending on the type of loading, each of these two structures becomes two halved substructures with different boundary conditions (at the intersection of the structure with its axis of symmetry). Finally, each of these two substructures is analyzed separately, and their responses are appropriately combined to obtain the main structure response. Three symmetric structures are used to demonstrate the efficacy, speed, and accuracy of the proposed approach, and the results are compared to those obtained using the direct method. The first problem involves calculating and comparing the time required to analyze symmetrical frames with various numbers of bays and stories. The results show that the time difference between the two analysis methods increases with increasing the number of bays and stories, which increases the structural degree of freedom and dimensions of the problem. To assess the proposed approach in the RBDO problem, the 3-bay 15-story symmetric frame and 200bar symmetric planar truss are investigated. As the result of these two problems displays, the proposed approach reduces the dimensions of matrices that must be inverted, the data stored in memory, and the computational time. In addition, compared to the direct method, the proposed approach requires significantly less computational time to solve the RBDO problem using EVPS. This time reduction varies according to the type of symmetry, geometry, and dimensions of the structure. For example, utilizing the direct structural analysis method for structural analysis to determine the best solution for the RBDO problem on a 200bar symmetric planar truss with 10 independent runs takes 229 hours (approximately 1.98% longer than the proposed approach). This time would be 1,380 hours (about 37% longer than the proposed approach) in the 3-bay 15-story symmetric frame.

### References

- [1] Kangwai R, Guest S (1999) Detection of finite mechanisms in symmetric structures. International Journal of Solids and Structures 36(36):5507-5527.
- [2] Kangwai R, Guest S, Pellegrino S (1999) An introduction to the analysis of symmetric structures. Computers and structures 71(6):671-688.
- [3] Kangwai R, Guest S (2000) Symmetry-adapted equilibrium matrices. International Journal of Solids and Structures 37(11):1525-1548.
- [4] Harth P, Michelberger P (2016) Determination of loads in quasi-symmetric structure with symmetry components. Engineering Structures 123:395-407.
- [5] Harth P, Beda P, Michelberger P (2017) Static analysis and reanalysis of quasi-symmetric structure with symmetry components of the symmetry groups C3v and C1v. Engineering Structures 152:397-412.
- [6] Zhang P, Fan W, Chen Y, Feng J, Sareh P (2022) Structural symmetry recognition in planar structures using Convolutional Neural Networks. Engineering Structures 260:114227.
- [7] Chen Y, Feng J, Qian Z (2016) A self-equilibrated load method to locate singular configurations of symmetric foldable structures. Acta Mechanica 227(10):2749-2763.
- [8] Kaveh A, Nikbakht M, Rahami H (2010) Improved group theoretic method using graph products for the analysis of symmetric-regular structures. Acta mechanica 210(3):265-289.
- [9] Kaveh A, Jahanmohammadi A (2008) Grouptheoretic method for forced vibration analysis of symmetric structures. Acta mechanica 199(1):1-16.
- [10] Kaveh A, Fazli H (2007) Graph coloration and group theory for factorization of symmetric dynamic systems. Acta mechanica 192(1):111-133.
- [11] Kaveh A, Nikbakht M (2008) Stability analysis of hyper symmetric skeletal structures using group theory. Acta mechanica 200(3):177-197.
- [12] Zingoni A (2012) Symmetry recognition in grouptheoretic computational schemes for complex structural systems. Computers and Structures 94:34-44.

- [13] Chen Y, Feng J (2012) Generalized eigenvalue analysis of symmetric prestressed structures using group theory. Journal of Computing in Civil Engineering 26(4):488-497.
- [14] Kaveh A, Rahami H (2011) Block circulant matrices and applications in free vibration analysis of cyclically repetitive structures. Acta Mechanica 217(1):51-62.
- [15] Kaveh A, Rahami H (2007) Tri-diagonal and penta-diagonal block matrices for efficient eigensolutions of problems in structural mechanics. Acta Mechanica 192(1):77-87.
- [16] Kaveh A, Rahami H (2007) Compound matrix block diagonalization for efficient solution of eigenproblems in structural mechanics. Acta Mechanica 188(3):155-166.
- [17] Kaveh A, Sayarinejad M (2003) Eigensolutions for matrices of special structures. Communications in Numerical Methods in Engineering 19(2):125-136.
- [18] Kaveh A, Sayarinejad M (2004) Graph symmetry and dynamic systems. Computers and Structures 82 (23-26):2229-2240.
- [19] Kaveh A, Nikbakht M (2006) Buckling load of symmetric plane frames using canonical forms and group theory. Acta mechanica 185(1):89-128.
- [20] Kaveh A, Rahami H (2004) A new spectral method for nodal ordering of regular space structures. Finite Elements in Analysis and Design 40 (13-14):1931-1945.
- [21] Kaveh A, Sayarinejad M (2006) Eigensolution of specially structured matrices with hypersymmetry. International journal for numerical methods in engineering 67(7):1012-1043.
- [22] Kaveh A, Sayarinejad M (2006) Additivity properties of graphs with Form II symmetry. Communications in numerical methods in engineering 22(3):181-195.
- [23] Kaveh A, Salimbahrami B (2007) Buckling load of symmetric plane frames using canonical forms. Computers and Structures 85 (17-18):1420-1430.
- [24] Kaveh A, Rahami H (2005) New canonical forms for analytical solution of problems in structural mechanics. Communications in Numerical Methods in Engineering 21(9):499-513.
- [25] Kaveh A, Rahami H (2004) An efficient method for decomposition of regular structures using graph products. International Journal for Numerical Methods in Engineering 61(11):1797-1808.

- [26] Meng Z, Zhou H, Li G, Hu H (2017) A hybrid sequential approximate programming method for second-order reliability-based design optimization approach. Acta Mechanica 228(5):1965-1978.
- [27] Nikolaidis E, Burdisso R (1988) Reliability based optimization: a safety index approach. Computers and Structures 28(6):781-788.
- [28] Dubourg V, Sudret B, Bourinet J-M (2011) Reliability-based design optimization using kriging surrogates and subset simulation. Structural Multidisciplinary Optimization 44(5):673-690.
- [29] Shan S, Wang GG (2008) Reliable design space and complete single-loop reliability-based design optimization. Reliability Engineering and System Safety 93(8):1218-1230.
- [30] Schuëller GI, Jensen HA (2008) Computational methods in optimization considering uncertainties—an overview. Computer Methods in Applied Mechanics and Engineering 198(1):2-13.
- [31] Cheng K, Lu Z, Xiao S, Zhang X, Oladyshkin S, Nowak W (2021) Resampling method for reliability-based design optimization based on thermodynamic integration and parallel tempering. Mechanical systems and signal processing 156:107630.
- [32] Kaveh A, Hoseini Vaez SR, Hosseini P, Fathali MA (2021) Heuristic operator for reliability assessment of frame structures. J Periodica Polytechnica Civil Engineering 65(3):702-716.
- [33] Mazdarani MJH, Hoseini Vaez SR, Hosseini P, Fathali MA Reliability-based layout optimization of concentrically braced in 3D steel frames. In: Structures, 2023. Elsevier, pp 1094-1112.
- [34] Hoseini Vaez SR, Mehanpour H, Fathali MA (2020) Reliability assessment of truss structures with natural frequency constraints using metaheuristic algorithms. Journal of Building Engineering 28:101065.
- [35] Hoseini Vaez SR, Fathali MA, Mehanpour H (2022) A two-step approach for reliability-based design optimization in power transmission line towers. International Journal on Interactive Design and Manufacturing:1-25.
- [36] Hosseini P, Hoseini Vaez H, Fathali M, Mehanpour H (2020) Reliability Assessment of Transmission Line Towers Using Metaheuristic Algorithms. Int J Optim Civil Eng 10(3):531-551.
- [37] Hoseini Vaez SR, Hosseini P, Fathali M, Samani A, Kaveh A (2020) Size and shape reliability-based

- optimization of dome trusses. Int J Optim Civil Eng 10(4):701-714
- [38] Paknahad M, Hosseini P, Kaveh A (2023) A self-adaptive enhanced vibrating particle system algorithm for continuous optimization problems. Int J Optim Civl Eng 13(1):127-142.
- [39] Kaveh A, Dadras Eslamlou A, Kaveh A, Dadras Eslamlou A (2020) Optimal design of steel curved roof frames by enhanced vibrating particles system algorithm. Metaheuristic optimization algorithms in civil engineering: new applications:73-97.
- [40] Hosseini P, Kaveh A, Hoseini Vaez SR (2022) Robust design optimization of space truss structures. Int J Optim Civ Eng 12:595-608.
- [41] Kaveh A, Ghazaan MI (2017) A new metaheuristic algorithm: vibrating particles system. Scientia Iranica Transaction A, Civil Engineering 24(2):551.
- [42] Kaveh A, Hoseini Vaez SR, Hosseini P (2019) Enhanced vibrating particles system algorithm for damage identification of truss structures. Scientia Iranica Transaction A, Civil Engineering 26(1):246-256.
- [43] Talatahari S, Gandomi AH, Yang X-S, Deb S (2015) Optimum design of frame structures using the eagle strategy with differential evolution. Engineering Structures 91:16-25.
- [44] Kaveh A, Ghafari M, Gholipour Y (2017) Optimum seismic design of steel frames considering the connection types. Journal of Constructional Steel Research 130:79-87.
- [45] AISC-LRFD (2001) Load and Resistance Factor Design Specification for Structural Steel Buildings, American Institute of Steel Construction Inc., Chicago (IL).
- [46] Ho-Huu V, Nguyen-Thoi T, Vo-Duy T, Nguyen-Trang T (2016) An adaptive elitist differential evolution for optimization of truss structures with discrete design variables. Computers and Structures 165:59-75.
- [47] Sonmez M (2011) Artificial Bee Colony algorithm for optimization of truss structures. Applied Soft Computing 11(2):2406-2418.
- [48] Toğan V, Daloğlu AT (2008) An improved genetic algorithm with initial population strategy and self-adaptive member grouping. Computers and Structures 86 (11-12):1204-1218.